A spectroscopic study of the E 1Σ+ g and F 1Σ+ g states of 7Li2 by pulsed optical–optical double resonance

R. A. Bernheim, L. P. Gold, P. B. Kelly, C. Tomczyk, and D. K. Veirs

Citation: The Journal of Chemical Physics **74**, 3249 (1981); doi: 10.1063/1.441529
View online: http://dx.doi.org/10.1063/1.441529
View Table of Contents: http://scitation.aip.org/content/aip/journal/jcp/74/6?ver=pdfcov
Published by the AIP Publishing

A spectroscopic study of the $E\,^1\Sigma_g^+$ and $F\,^1\Sigma_g^+$ states of $^7Li_2$ by pulsed optical–optical double resonance

R. A. Bernheim, L. P. Gold, P. B. Kelly, C. Tomczyk, and D. K. Veirs

Department of Chemistry, Davey Laboratory, The Pennsylvania State University, University Park, Pennsylvania 16802

(Received 7 November 1980; accepted 25 November 1980)

The results of pulsed optical–optical double resonance spectroscopic studies of the $E\,^1\Sigma_g^+$ and $F\,^1\Sigma_g^+$ states of $^7Li_2$ are presented. Observations were carried out on the $v^* = 0$ through $v^* = 30$ levels of the $F\,^1\Sigma_g^+$ state, representing about 60% of the dissociation energy. A set of Dunham molecular constants was derived and an RKR potential was generated. Franck–Condon factors were determined for the range of observed vibrational levels. The spectroscopic results on the $E\,^1\Sigma_g^+$ state are preliminary and are included because of a probable homogeneous anticrossing between it and the $F\,^1\Sigma_g^+$ state. It is suggested that the $E\,^1\Sigma_g^+$ state correlates with the $(2\,^2S) + (3\,^2S)$ atomic lithium states while the $F\,^1\Sigma_g^+$ correlates with the $(2\,^2P) + (2\,^2P)$ states.

I. INTRODUCTION

It is by now well known that multiphoton excitation permits the study of molecular states that are forbidden by conventional one-photon absorption. Such techniques are of particular value to the study of homonuclear diatomic molecules where one half of the excited states are inaccessible by one-photon absorption from the ground state due to the selection rule for a required change in inversion symmetry for an electric dipole transition. Recently, pulsed optical–optical double resonance experiments on the $^7Li_2$ molecule were initiated with the intention of making a comprehensive spectroscopic investigation of the one-photon "forbidden" states in a molecule of fundamental interest.[1–3] The multiphoton technique of choice was optical–optical double resonance (OODR) where the molecular excitation is stepwise via a stable, well characterized intermediate energy level. Molecular fluorescence is used for detection. The flexibility of the OODR technique is significantly increased when two independently tunable lasers are used to produce the excitation, as was demonstrated for BaO using cw dye lasers.[4] In the experiments on $^7Li_2$ the added feature of using two independently tunable pulsed dye lasers was implemented. Among other advantages, this permits convenient control of the amount of relaxation among the levels of the intermediate state by suitably delaying the second laser pulse in the OODR sequence. The resulting band spectra can be readily and unambiguously assigned.

Li_2 is a particularly important molecule for study as it is the least complex stable homonuclear diatomic molecule with the exception of molecular hydrogen. As such it has received considerable experimental and theoretical attention, being the subject of over 100 publications.[5] Nevertheless, most of the lower excited electronic states of Li_2 have never been observed, and uncertainties surround some of the states that have been carefully studied. For example, a large amount of experimental effort has been expended on the $X\,^1\Sigma_g^+$ ground state, and while many of the molecular constants of this state are very precisely known, some uncertainty remains in the $X\,^1\Sigma_g^+$ dissociation energy.[6] Of the first group of excited states which correlate with the $(2\,^2S) + (2\,^2P)$ atomic lithium states, six are predicted to be stable,[7,8] but only two ($A\,^1\Sigma_u^+$ and $B\,^1\Pi_u$) have been observed and characterized.[5,9] Of the electronic states that fall at energies higher than this first group, fragmentary evidence exists for only two ($C\,^1\Pi_u$ and $D\,^1\Pi_u$).[10–13] The present program of OODR experiments on $^7Li_2$ has resulted in the discovery of eight new electronic states.

Among the recently discovered excited singlet *gerade* states of Li_2, the lower 60% of the $G\,^1\Pi_g$ is known with reasonable accuracy and includes the first 20 vibrational levels.[3] The present paper presents a careful analysis of the $F\,^1\Sigma_g^+$ state for which preliminary results were previously reported.[2] A small portion of the $E\,^1\Sigma_g^+$ state has been observed and is included in this discussion as there apparently exists an interesting homogeneous anticrossing between it and the $F\,^1\Sigma_g^+$ state. A set of Dunham molecular constants is derived for the $F\,^1\Sigma_g^+$ state as well as an RKR potential curve and Franck–Condon factors for the transitions from the $A\,^1\Sigma_u^+$ state. The data and analysis cover the range of vibrational levels from $v^* = 0$–30.

While the vibrational numbering remains to be confirmed for the $E\,^1\Sigma_g^+$ state, the preliminary assignments of the pulsed OODR experiments indicate that the range of observed levels is $v^* = 1$–4. Molecular constants for this state based upon this limited data are presented.

The anticrossing between the $F\,^1\Sigma_g^+$ and a neighboring $^1\Sigma_g^+$ state is revealed by the negative value of $\alpha = -Y_{11}$ and the maximum in the observed B_v vs v curve. It is suggested that the perturbing $^1\Sigma_g^+$ state is the $E\,^1\Sigma_g^+$ state.

II. EXPERIMENTAL

The experimental arrangement for the investigation of $^7Li_2$ by pulsed OODR has been described earlier[1,3] and is only briefly summarized here. The Li sample was contained in a cruciform heat pipe oven which was also initially filled with about 30 Torr of helium at room temperature. The center of the cell was operated at approximately 800 °C while the arms remained at room temperature. Rough estimates of the partial pressures of the species present in the center of the heat pipe oven where the measurements were made are 70 Torr He, 0.1 Torr Li_2, and 2.6 Torr Li. The OODR excitation

 0021-9606/81/063249-06$01.00

was produced by two pulsed dye lasers. $X\,^1\Sigma_g^+$ ground state Li_2 molecules were first excited to the $A\,^1\Sigma_u^+$ state by a pump laser constructed according to the design of Hänsch.[14] Excitation from the $A\,^1\Sigma_u^+$ state to higher *gerade* states was produced by a probe dye laser (Molectron DL-300). Both pump and probe dye lasers were operated without etalon tuning elements, and both produced radiation linewidths of 0.3 cm^{-1}. Both dye lasers were pumped by the divided output beam of a Molectron UV-1000 nitrogen laser operating at 10 pulses per sec and producing 700 kW at 337.1 nm. $A\,^1\Sigma_u^+ - X\,^1\Sigma_g^+$ pump transitions were selected which were strong, unambiguously assigned, and not overlapped with other transitions. The probe laser wavelength was scanned, and the vibrational bands arising from excitation to the $E\,^1\Sigma_g^+$ and $F\,^1\Sigma_g^+$ states were detected by monitoring the molecular fluorescence from the heat pipe cell. Excitation of the upper portion of the $F\,^1\Sigma_g^+$ state was detected by monitoring ultraviolet fluorescence. In a separate experiment a single tunable cw dye laser was used to populate the $F\,^1\Sigma_g^+$ state via an OODR transition requiring light of only one wavelength. The ultraviolet fluorescence produced in this experiment was dispersed with a Spex 1401 monochromator and found to originate from the $C\,^1\Pi_u$ state, presumably populated by collisional transfer. In other pulsed experiments, excitation of the lower portions of the $F\,^1\Sigma_g^+$ state and the $E\,^1\Sigma_g^+$ state was detected by observation of fluorescence in the 380–580 nm range.[15]

The powers at which the pump and probe lasers were operated depended upon which intermediate levels were chosen for excitation and upon the gain curves of the various dyes used. The pump laser was operated between 0.02 and 0.15 mJ/pulse. The lower powers were used with easily populated intermediate levels, e.g., $A\,^1\Sigma_u^+ (v=1)$, which permitted the probe laser to be operated at higher power levels. With less easily populated intermediate levels, including the higher vibrational levels of the $A\,^1\Sigma_u^+$ state, more pump power was needed. The probe dye laser was operated so as to deliver between 0.02 and 0.3 mJ/pulse, depending upon the requirements of the pump laser, the type of dye used, and the region of the dye gain curve utilized.

Upon suitable optical delay of the arrival of the probe laser pulse at the sample cell, rotational relaxation of the $A\,^1\Sigma_u^+$ state takes place, and the subsequent excitation to the $E\,^1\Sigma_g^+$ and $F\,^1\Sigma_g^+$ states consists of bands of rotational spectral lines. Rotational transfer up to $\Delta J = 30$ was observed in the $A\,^1\Sigma_u^+$ state in these experiments.

Calibration of the OODR spectrum was achieved by simultaneously recording the spectra of neon and argon produced in optogalvanic cells and the fringes produced when part of the probe laser radiation was sampled by a Fabry-Perot interferometer. The OODR spectral line positions could be determined with an estimated accuracy of 0.2 cm^{-1}.

III. OBSERVED SPECTRA AND ANALYSIS

Transitions to the $E\,^1\Sigma_g^+$ and $F\,^1\Sigma_g^+$ states from selected levels of the $A\,^1\Sigma_u^+$ state of $^7Li_2$ were observed. The measured wavelengths for all experiments were converted to energies all referred to the bottom of the $A\,^1\Sigma_u^+$ state potential well using the known $A\,^1\Sigma_u^+$ state molecular constants.[9] After assignment of the vibrational and rotational quantum numbers v^* and J^*, the two sets of data $E\,^1\Sigma_g^+ (v^*, J^*)$ and $F\,^1\Sigma_g^+ (v^*, J^*)$ were fitted with molecular constants.

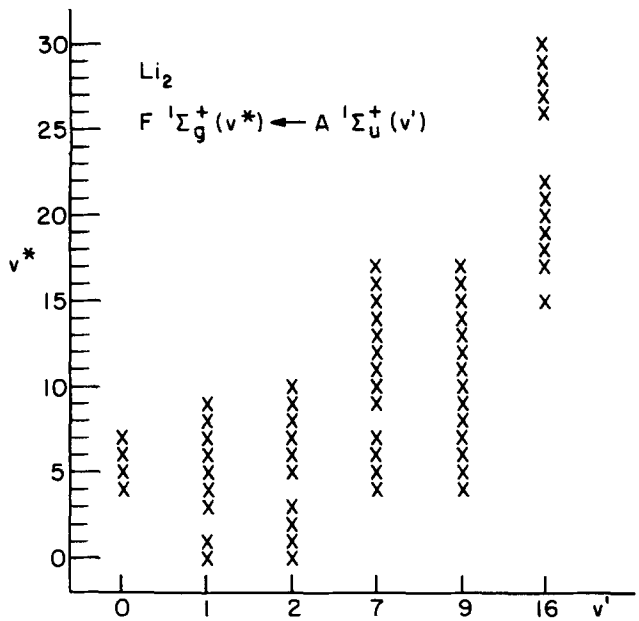

FIG. 1. The range of vibrational states v^* found in the $F\,^1\Sigma_g^+$ state using different levels v', J' of the $A\,^1\Sigma_u^+$ intermediate state. The observations for $v'=0$ and $v'=2$ were only used to verify the vibrational state numbering v^*, while the remaining data were used in the generation of molecular constants of the $F\,^1\Sigma_g^+$ state. It should be noted that these observations were incomplete below $v^*=4$ for $v'=0$, $v^*=4$ for $v'=7$, $v^*=$ is for $v'=16$, and above for $v^*=17$ for $v'=9$.

A. The $F\,^1\Sigma_g^+$ state

For the $F\,^1\Sigma_g^+$ state 1105 transitions were assigned, of which 981 were used in the final spectral fit. The rotational assignments are trivial as described previously. The vibrational assignments were made on the basis of a number of experiments as well as comparisons for consistency of the observed band intensities with calculated Franck–Condon factors. Experimentally, the vibrational levels pumped in the $A\,^1\Sigma_u^+$ state were $v'=0$, 1, 2, 7, 9, and 16. The resulting $F\,^1\Sigma_g^+$ state vibrational levels v^* which were excited from each intermediate v' state are shown in Fig. 1. No bands below that assigned to $v^*=0$ were observed when the $v'=1$ and $v'=2$ levels of the $A\,^1\Sigma_u^+$ state were pumped. The missing bands at $v^*=2$ when $v'=1$ was pumped, at $v^*=8$ when $v'=7$ was pumped, and at $v^*=16$, 23, 24, and 25 when $v'=16$ was pumped are all consistent with the negligible Franck–Condon factors for these transitions as are the relative intensities of the observed bands. Spectra were observed which corresponded to transitions to energy levels in the range of 30 000–35 000 cm^{-1} above the ground state.

Following the assignments of v^* and J^*, the data were fitted by a least squares method with an equation of the form

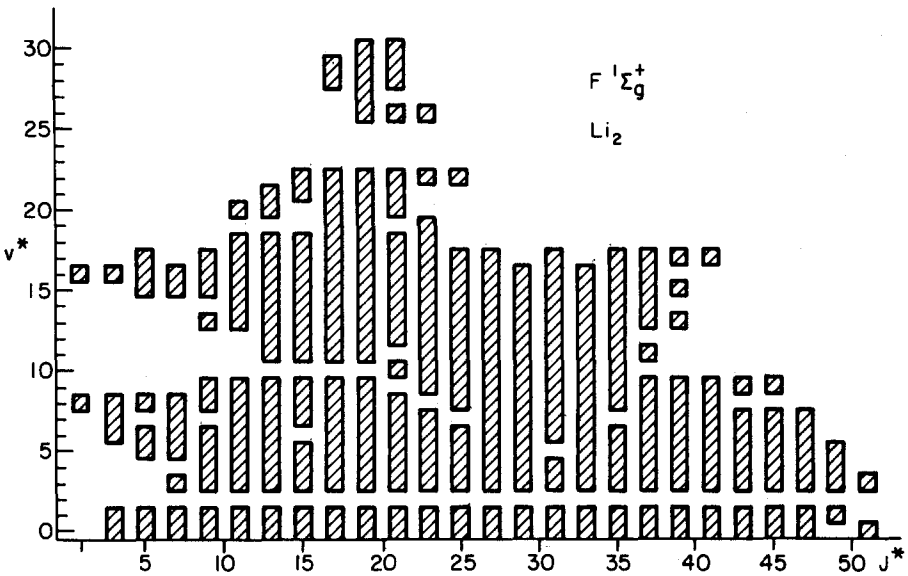

FIG. 2. The data field of values of v^* and J^* for the $F\,^1\Sigma_g^+$ levels used in the evaluation of the molecular constants.

$$\nu(v,J)=\sum_{n,k} Y_{nk}(v+\tfrac{1}{2})^n[J(J+1)]^k\ . \tag{1}$$

Preliminary analyses served to eliminate perturbed lines and transitions to other states. In the final analysis 17 constants were fitted to 981 observed transitions.[16] The range of vibrational and rotational levels for the data used in the fit are shown in Fig. 2. It will be noted that the data field includes only odd values of J^*. This is a result of choosing an even value of J' in each of the vibrational levels which were pumped in the $A\,^1\Sigma_u^+$ state. The standard error of the least squares fit was 0.15 cm^{-1}, which is consistent with the precision of measurement. The molecular constants obtained from the fit are given in Table I. In general, more significant figures are listed than would apparently be justified by the determined standard error. Nevertheless, in some cases the extra digits are necessary due to the effects of correlation between the different Dunham coefficients.[17] The value of T_e is referred to the bottom of the $X\,^1\Sigma_g^+$ ground state potential by using the value of $1.406\,830\,7\times10^4$ cm^{-1} found for the bottom of the $A\,^1\Sigma_u^+$ state well.[9]

The observed value of $Y_{02}=-4.06\times10^{-6}$ cm^{-1} differs by about 5% from the value of -4.28×10^{-6} cm^{-1} calculated for the relation

$$Y_{02}=4Y_{01}^3/Y_{10}^2\ , \tag{2}$$

which is the mean contribution from the influence of centrifugal force for the vibrationless molecule. The effect of vibration on the centrifugal distortion is several times larger than that found for the $G\,^1\Pi_g$ state.[3]

The molecular constants in Table I were used to calculate[18] a Rydberg–Klein–Rees (RKR) potential curve which is given in Table II together with the values of

$$G_v=\sum_{n=1} Y_{n0}(v+\tfrac{1}{2})^n\ , \tag{3}$$

and

$$B_v=\sum_{n=0} Y_{n1}(v+\tfrac{1}{2})^n\ , \tag{4}$$

found from the constants in Table I.

Franck–Condon factors for the excitation from the $A\,^1\Sigma_u^+$ state were calculated[18] from the RKR curve. The results, given in Table III, are in good agreement with observation, confirming the $F\,^1\Sigma_g^+$ state vibrational assignments.

In our study of the $G\,^1\Pi_g$ state of $^7Li_2$ it was concluded that the state correlated with the $(2\,^2P)+(2\,^2P)$ atomic lithium states in the dissociation limit. The energies of the two $^1\Sigma_g^+$ states in the present study fall below that of the $G\,^1\Pi_g$ state, with the $F\,^1\Sigma_g^+$ state having a higher energy than the $E\,^1\Sigma_g^+$ state. There are two possibilities:

TABLE I. The Dunham coefficients that describe the $F\,^1\Sigma_g^+$ state of $^7Li_2$ from $v^*=0$–30. The quantities in parentheses are the exponents of 10 in the multiplying factor, and all values are in cm^{-1}.

n,k	$Y_{n,k}(F\,^1\Sigma_g^+)$	Standard error
T_e	2.997 497 8 (+4)	6.5 (−2)
1,0	2.272 542 3 (+2)	8.3 (−2)
2,0	−2.472 309 4 (0)	4.0 (−2)
3,0	6.209 599 6 (−2)	9.0 (−3)
4,0	1.624 265 9 (−3)	1.1 (−3)
5,0	−6.345 680 1 (−4)	7.5 (−5)
6,0	4.139 683 4 (−5)	2.9 (−6)
7,0	−1.100 683 7 (−6)	6.1 (−8)
8,0	1.063 613 8 (−8)	5.1 (−10)
0,1	3.817 736 7 (−1)	1.3 (−5)
0,2	−4.435 405 7 (−6)	1.0 (−8)
0,3	1.375 019 8 (−10)	2.4 (−11)
1,1	3.829 570 1 (−3)	3.2 (−5)
2,1	−5.308 724 0 (−4)	2.9 (−6)
3,1	1.059 450 3 (−5)	8.1 (−8)
1,2	−4.627 915 1 (−7)	1.1 (−8)
2,2	1.964 957 3 (−8)	6.9 (−10)

TABLE II. G_v values, rotational constants B_v, and RKR potential curve for the $F\,^1\Sigma_g^+$ state of $^7Li_2$ for $J=0$.

v	G_v (cm^{-1})[a]	B_v (cm^{-1})[a]	r_{min} (Å)	r_{max} (Å)
−1/2	0	0.381 773 7	3.54789	
0	113.017	0.383 557 1	3.341 74	3.754 89
1	335.532	0.386 359 3	3.190 55	3.912 33
2	553.665	0.388 195 2	3.087 70	4.027 14
3	767.746	0.389 128 2	3.005 92	4.126 14
4	978.038	0.389 222 0	2.937 23	4.216 94
5	1184.722	0.388 540 1	2.877 88	4.302 95
6	1387.903	0.387 146 1	2.825 70	4.386 07
7	1587.622	0.385 103 5	2.779 27	4.467 48
8	1783.868	0.382 375 9	2.737 57	4.547 96
9	1976.606	0.379 326 8	2.699 85	4.628 08
10	2165.795	0.375 720 0	2.665 52	4.708 23
11	2351.404	0.371 718 8	2.634 15	4.788 66
12	2533.432	0.367 386 9	2.605 37	4.869 50
13	2711.919	0.362 787 8	2.578 90	4.950 80
14	2886.947	0.357 985 2	2.554 52	5.032 51
15	3058.647	0.353 042 5	2.532 03	5.115 42
16	3227.184	0.348 023 4	2.511 27	5.196 66
17	3392.753	0.342 991 4	2.492 10	5.278 74
18	3555.558	0.338 010 1	2.474 32	5.360 58
19	3715.793	0.333 143 0	2.457 83	5.442 01
20	3873.623	0.328 453 7	2.442 36	5.522 95
21	4029.164	0.324 005 8	2.427 70	5.603 38
22	4182.462	0.319 862 8	2.413 57	5.683 38
23	4333.484	0.316 088 4	2.399 68	5.763 16
24	4482.120	0.312 756 0	2.385 70	5.842 95
25	4628.192	0.309 899 3	2.371 30	5.923 05
26	4771.486	0.307 611 8	2.356 16	6.003 70
27	4911.804	0.305 947 1	2.340 04	6.084 98
28	5049.048	0.304 968 7	2.322 80	6.166 57
29	5183.332	0.304 740 3	2.304 52	6.247 54
30	5315.136	0.305 325 3	2.285 57	6.325 91

[a]Calculated from Eqs. (3) and (4) and the constants in Table I.

(1) either both the $E\,^1\Sigma_g^+$ and $F\,^1\Sigma_g^+$ states also correlate with the $(2\,^2P)+(2\,^2P)$ atomic lithium states, or (2) the $E\,^1\Sigma_g^+$ state correlates with the lower energy $(2\,^2S)+(3\,^2S)$ atomic lithium states and the $F\,^1\Sigma_g^+$ state correlates with the $(2\,^2P)+(2\,^2P)$ atomic lithium states. Correlation of the $F\,^1\Sigma_g^+$ state with the $(2\,^2S)+(3\,^2S)$ atomic lithium states can be ruled out on purely energetic grounds, aside from the fact that the $E\,^1\Sigma_g^+$ state lies immediately below in energy. The relationship of the $E\,^1\Sigma_g^+$, $F\,^1\Sigma_g^+$, and $G\,^1\Pi_g$ states to each other and to the dissociated atom states can be seen in Fig. 3. The dissociation energies of the $E\,^1\Sigma_g^+$ and $F\,^1\Sigma_g^+$ states are not sufficiently well known to provide for an exact assignment. Nevertheless, all of the presently known facts indicate that the $F\,^1\Sigma_g^+$ state correlates with the $(2\,^2P)+(2\,^2P)$ atomic lithium states. At energies above the $E\,^1\Sigma_g^+$, $F\,^1\Sigma_g^+$, and $G\,^1\Pi_g$ states, five additional *gerade* states have been observed in the present experiments. Accepting a recent value of $D_e = 8516 \pm 18$ cm^{-1} for the $X\,^1\Sigma_g^+$ ground state,[19] which is within the limits of the best published estimate[6] of $D_e = 8450 \pm 100$ cm^{-1}, one arrives at a value of $D_e = 8349$ cm^{-1} for the $F\,^1\Sigma_g^+$ state.

In Fig. 4 the B_v values of the $F\,^1\Sigma_g^+$ state are plotted as a function of v. The maximum of B_v at $v=5$ should be noted. This unusual behavior is also reflected in the positive sign for the Y_{11} Dunham constant in Eq. (1). This means that the lower portion of the potential energy curve for the $F\,^1\Sigma_g^+$ state increases more rapidly with increasing internuclear distance than with decreasing internuclear distance for the lower vibrational levels. This feature is compatible with an avoided crossing with a nearby state. In this respect it is similar to the well-known avoided crossing in LiH which results in an increase

TABLE III. Franck–Condon factors ($\times 10^3$) for the $F\,^1\Sigma_g^+(v^*)$–$A\,^1\Sigma_u^+(v')$ transition of $^7Li_2$ for $J=0$.

v^* \ v'	0	1	2	3	4	5	6	7	8	9	10	11	12	13	14	15	16	17	18	19	20
0	114	287	317	196	71	14	1														
1	248	151	1	156	253	147	39	4													
2	272	1	137	59	33	219	202	69	9												
3	197	73	78	35	111		159	235	98	14											
4	105	167		108		107	13	104	249	126	19										
5	44	160	72	25	79	14	77	39	62	252	152	25									
6	15	97	142	13	61	38	39	45	62	32	248	177	31								
7	4	44	129	91		75	10	59	20	79	13	237	199	38	1						
8	1	15	76	129	42	15	12		66	6	88	3	222	220	46	2					
9		4	33	101	106	11	35	50	4	64		91		203	139	55	3				
10			11	55	112	72		50	29	14	55	2	88	3	181	257	66	4			
11			3	23	76	107	40	4	55	12	26	42	8	80	11	155	272	79	6		
12			1	7	37	90	90	15	17	51	3	37	28	18	70	24	127	283	93	8	
13				2	14	54	96	66	2	30	40		43	16	29	56	41	98	291	110	11
14					4	25	69	92	40		39	26	3	45	7	41	42	59	69	293	128
15					1	9	37	79	79	19	7	43	14	11	42	1	50	27	78	44	289
16						3	16	50	83	60	5	17	40	5	19	36		57	14	95	24
17						1	6	25	62	79	39		27	33		27	27	3	60	5	108
18							2	10	36	70	69	20	2	33	22	1	32	18	9	60	
19								3	17	47	73	53	7	9	35	12	5	34	10	17	55
20								1	7	26	57	70	36	1	18	33	5	11	33	4	26
21									2	12	36	63	61	20	1	25	26	1	18	29	1
22										4	18	45	65	48	8	5	29	18		24	23
23										1	8	27	53	62	33	2	12	29	10	3	27
24											3	13	35	58	54	20		18	26	4	8
25											1	6	20	44	60	44	9	2	23	20	1
26												2	9	27	50	57	32	3	7	24	13
27												1	4	14	35	55	51	21		12	22
28													1	6	20	42	56	43	12		15
29														2	10	27	48	55	34	6	2
30														1	4	14	34	53	51	25	2

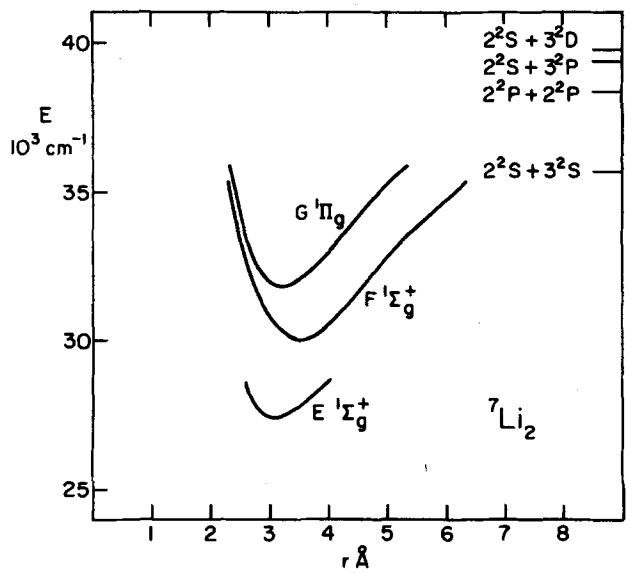

FIG. 3. Potential curves for the lowest three excited *gerade* electronic states of $^7Li_2$ observed in this study and their relationship to the separated atomic states. The energies are referred to the bottom of the $X\,^1\Sigma_g^+$ ground state potential well.

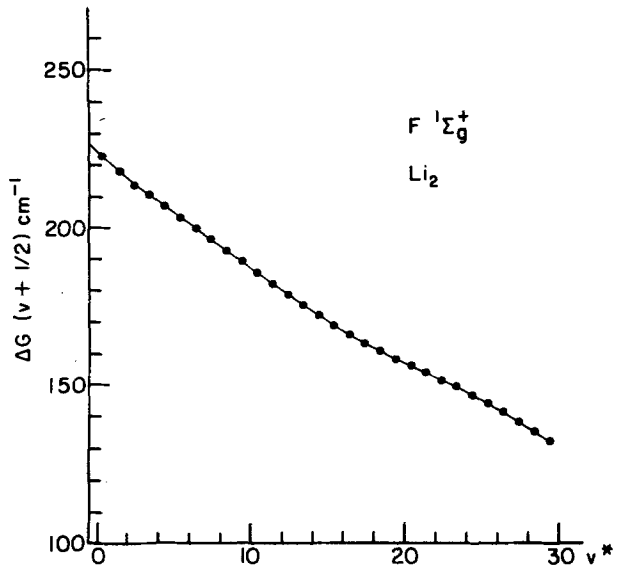

FIG. 5. The variation of $\Delta G\,(v+\frac{1}{2})$ with vibrational quantum number v of the $F\,^1\Sigma_g^+$ state.

of B_v values for the $A\,^1\Sigma_u^+$ state of that molecule before the normal decrease sets in.[20] The perturbation appears to be homogeneous, affecting the rotational levels of lower vibrational states uniformly. Although the observations do not include the $J^* = 0$ states, the perturbation extends over many vibrational levels of $F\,^1\Sigma_g^+$. For such a homogeneous perturbation the interacting state must also be a $^1\Sigma_g^+$ state.[21] It is suggested that the state responsible for the perturbation is the $E\,^1\Sigma_g^+$ state, although at present there is no corroboration from observations of $E\,^1\Sigma_g^+$ state levels. The observations on the higher $^1\Sigma_g^+$ states all occur at energies greater than the perturbation.

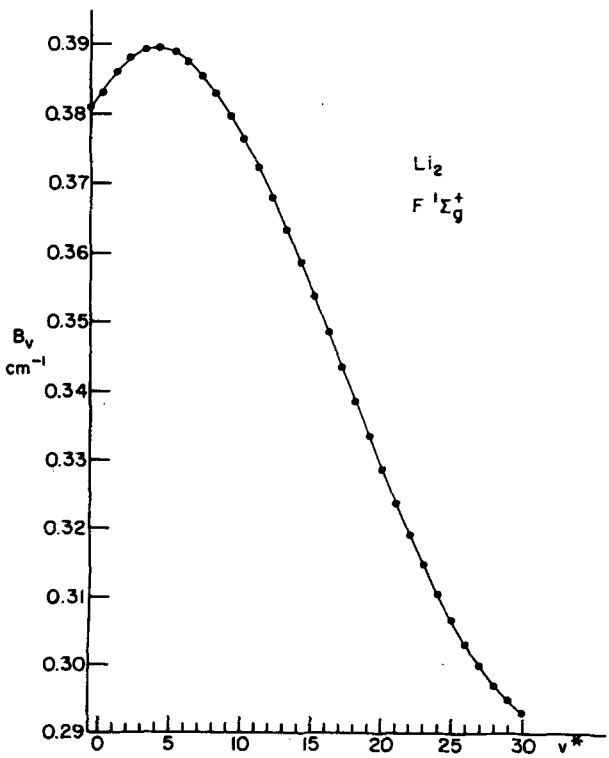

FIG. 4. The B_v values of the $F\,^1\Sigma_g^+$ state plotted as a function of vibrational quantum number v.

The $\Delta G(v+\frac{1}{2})$ curve shown in Fig. 5 also shows deviations from linearity near $v = 2$ and above $v = 16$. The sources of these irregularities have not been identified, although it is very likely that at least one of the interactions is the same as that responsible for the maximum in the B_v curve.

The equilibrium internuclear distance $r_e = 3.548$ Å is significantly larger than the value found for the other known states of $^7Li_2$ as shown in Table IV. It is also larger than the theoretical value for Li_2^+. This large value is consistent with the postulated anticrossing of the outer portion of the molecular potential with a lower state.

In addition to the homogeneous perturbation of the

TABLE IV. Summary of selected molecular constants for $^7Li_2$.

State	T_e (cm^{-1})	ω_e (cm^{-1}) (Y_{10})	B_e (cm^{-1}) (Y_{01})	r_e (Å)	Footnote
$G\,^1\Pi_g$	31 868.45	229.26	0.468 87	3.201 4	a
$F\,^1\Sigma_g^+$	29 975.12	227.25	0.381 77	3.547 9	b
$E\,^1\Sigma_g^+$	27 652	239.9	0.495	3.12	b
$D\,^1\Pi_u$	34 518	201.68	0.462 8	3.222	c
$C\,^1\Pi_u$	30 550.6	237.9	0.507 5	3.077	c
$B\,^1\Pi_u$	20 436.33	270.66	0.557 37	2.936 3	d
$A\,^1\Sigma_u^+$	14 068.31	255.47	0.497 42	3.108 2	e
$X\,^1\Sigma_g^+$	0	351.42	0.672 45	2.673 3	e

[a]Reference 3.
[b]This work.
[c]Reference 22.
[d]Reference 5.
[e]Reference 9.

TABLE V. Preliminary molecular constants which describe the $E\,^1\Sigma_g^+$ state of $^7Li_2$ derived from what are thought to be the $v^* = 1$–4 vibrational states. The quantities in parenthesis are the exponents of 10 in the multiplying factor, and all values are in cm^{-1}.

n, k	$Y_{n,k}$ ($E\,^1\Sigma_g^+$)	Standard error
T_e	2.740 565 1 (+4)	4.2 (−1)
1,0	2.518 885 7 (+2)	2.3 (−1)
2,0	−6.002 446 0 (0)	4.5 (−2)
0,1	5.076 174 5 (−1)	1.2 (−3)
0,2	−6.818 512 7 (−6)	1.2 (−6)
1,1	−1.261 024 4 (−2)	3.4 (−4)
1,2	−8.645 082 3 (−7)	2.7 (−7)

$F\,^1\Sigma_g^+$ state, a number of inhomogeneous perturbations were observed and are listed in supplementary tables.[16]

B. The $E\,^1\Sigma_g^+$ state

Only a small portion of the $E\,^1\Sigma_g^+$ state was observed in these pulsed OODR experiments. While the rotational assignments are unambiguous as described previously, the vibrational assignment is less certain. The data set, consisting of 41 transitions, includes only four vibrational states when the $v' = 0$, 1, and 2 states of the $A\,^1\Sigma_u^+$ state are used as intermediate pump levels. Franck–Condon factor calculations indicate that the observed vibrational states of the $E\,^1\Sigma_g^+$ state are $v^* = 1$–4. In a separate experiment, a two photon excitation spectrum was obtained with a single cw tunable dye laser (Coherent 490) operated with oxazine–I dye and pumped by a krypton ion laser. Although the resulting spectra are much more complex than those obtained in the pulsed experiments, it is evident that an additional vibrational state below those observed in the pulsed experiments was being excited. This lower vibrational state is presumably that with $v^* = 0$. Plans are underway to extend the "probe" pulsed dye laser to wavelengths beyond 750 nm to further study this state. Meanwhile, the molecular constants for the $E\,^1\Sigma_g^+$ state shown in Table V must be considered as preliminary until the vibrational assignment is confirmed and the data set extended to the upper portion of the $E\,^1\Sigma_g^+$ potential. By using the recent value of $D_e = 8516 \pm 18$ cm^{-1} for the $X\,^1\Sigma_g^+$ ground state dissociation energy,[19] one arrives at a value of $D_e \approx 8070$ cm^{-1} for the $E\,^1\Sigma_g^+$ state if it correlates with the $(2\,^2S) + (3\,^2S)$ atomic lithium states.

At present, insufficient data exist to attempt to obtain the interaction parameter for the perturbation or to obtain the "deperturbed" potential curves of the $F\,^1\Sigma_g^+$ and $E\,^1\Sigma_g^+$ states.

A summary of selected molecular constants for $^7Li_2$ is presented in Table IV for those states for which an analysis has been made. From the present work it appears that the lower 60% of the $F\,^1\Sigma_g^+$ state is known with reasonable accuracy and includes the first 30 vibrational levels. The previous OODR results on the $G\,^1\Pi_g$ state also covered the lower 60% of its potential curve. Besides the preliminary results reported here for the $E\,^1\Sigma_g^+$ state, the observations extend to what are apparently two additional $^1\Pi_g$ states and three additional $^1\Sigma_g^+$ states. The treatment of this additional data is in progress.

ACKNOWLEDGMENTS

This work has been supported in part by The National Science Foundation, and the Donors of The Petroleum Research Fund, administered by the American Chemical Society.

[1] R. A. Bernheim, L. P. Gold, P. B. Kelly, C. Kittrell, and D. K. Veirs, Phys. Rev. Lett. **43**, 123 (1979).
[2] R. A. Bernheim, L. P. Gold, P. B. Kelly, C. Kittrell, and D. K. Veirs, Chem. Phys. Lett. **70**, 104 (1980).
[3] R. A. Bernheim, L. P. Gold, P. B. Kelly, T. Tipton, and D. K. Veirs, J. Chem. Phys. (in press).
[4] R. A. Gottscho, J. B. Koffend, and R. W. Field, J. Chem. Phys. **68**, 4110 (1978).
[5] For a recent comprehensive review see M. M. Hessel and C. R. Vidal, J. Chem. Phys. **70**, 4439 (1979).
[6] D. D. Konowalow and M. L. Olson, J. Chem. Phys. **71**, 450 (1979).
[7] M. L. Olson and D. D. Konowalow, Chem. Phys. **22**, 29 (1977).
[8] D. K. Watson, C. J. Cerjan, S. Guberman, and A. Dalgarno, Chem. Phys. Lett. **50**, 181 (1977).
[9] P. Kusch and M. M. Hessel, J. Chem. Phys. **67**, 586 (1977).
[10] R. F. Barrow, N. Travis, and C. V. Wright, Nature (London) **187**, 141 (1960).
[11] R. Velasco, An. R. Soc. Esp. Fis. Quim. Ser. A **56**, 175 (1960).
[12] F. R. Rico, Opt. Pura Appl. **2**, 33 (1969).
[13] J. L. Mercier, F. R. Rico, and R. Velasco, Opt. Pura Appl. **2**, 96 (1969).
[14] T. W. Hänsch, Appl. Opt. **11**, 895 (1972).
[15] A color subtraction filter obtained from OCLI was used.
[16] See AIP document no. PAPS JCPSA-74-3249-27 for 27 pages containing observed spectral transitions, assignments, differences between observed and calculated spectral energies, and the variance–covariance and correlation matrix for the molecular constants. Order by PAPS number and journal reference from American Institute of Physics, Physics Auxiliary Publication Service, 335 East 45th Street, New York, N.Y. 10017. The price is $1.50 for microfiche or $5.00 for photocopies. Airmail is additional. Make check payable to the American Institute of Physics.
[17] D. L. Albritton, A. L. Schmeltekopf, and R. N. Zare, in *Molecular Spectroscopy: Modern Research*, edited by K. N. Rao (Academic, New York, 1976), Vol. II, p. 1.
[18] The computer programs used were developed by R. N. Zare and mentioned in W. Demtröder, M. McClintock, and R. N. Zare, J. Chem. Phys. **51**, 5495 (1969).
[19] K. K. Verma, M. E. Koch, and W. C. Stwalley (private communication).
[20] F. H. Crawford and T. Jorgensen, Jr., Phys. Rev. **47**, 932 (1935).
[21] G. Herzberg, *Molecular Spectra and Molecular Structure* (Van Nostrand, Princeton, N.J., 1950), 2nd edition, Vol. I.
[22] K. P. Huber and G. Herzberg, *Molecular Spectra and Molecular Structure* (Van Nostrand Reinhold, New York, 1979), Vol. IV.